ARTICLE

Check for updates

Generation of human A9 dopaminergic pacemakers from induced pluripotent stem cells

Hong Li[1,3], Houbo Jiang[1,2,3], Hanqin Li[1], Li Li[1], Zhen Yan [1,2] and Jian Feng [1,2 ✉]

The degeneration of nigral (A9) dopaminergic (DA) neurons causes motor symptoms in Parkinson's disease (PD). We use small-molecule compounds to direct the differentiation of human induced pluripotent stem cells (iPSCs) to A9 DA neurons that share many important properties with their in vivo counterparts. The method generates a large percentage of TH^{+} neurons that express appropriate A9 markers, such as GIRK2 and ALDH1A1, but mostly not the A10 marker CALBINDIN. Functionally, they exhibit autonomous pacemaking based on L-type voltage-dependent Ca^{2+} channels and show autoreceptor-dependent regulation of dopamine release. When transplanted in the striatum of 6-OHDA-lesioned athymic rats, the human A9 DA neurons manifest robust survival and axon outgrowth, and ameliorate motor deficits in the rat PD model. The ability to generate patient-specific A9 DA autonomous pacemakers will significantly improve PD research and facilitate the development of disease-modifying therapies.

Molecular Psychiatry; https://doi.org/10.1038/s41380-022-01628-1

INTRODUCTION

Midbrain dopaminergic (DA) neurons are categorized into three groups (A8, A9 and A10) based on the location of their somas and projection patterns [1, 2]. A9 DA neurons, which reside in the substantia nigra and project to the dorsal lateral striatum with their massive axon arborizations [3], exhibit a fairly selective loss in Parkinson's disease (PD), while A8 and A10 groups of DA neurons are largely spared [4]. A9 DA neurons express markers such as ALDH1A1 and GIRK2 [5], but largely not CALBINDIN, which is expressed in A10 DA neurons [6]. Transplantation of mouse A9, but not A10, DA neurons in 6-OHDA-lesioned rat striatum supports graft survival, fiber outgrowth and recovery of motor symptoms [5, 7]. Nigral DA neurons fire action potentials spontaneously even in the absence of synaptic inputs [8]; these autonomous pacemaking action potentials ensure a steady release of dopamine, which is necessary for the balanced actions of direct and indirect pathways that control locomotion [9, 10].

Because of the importance of nigral DA neurons in Parkinson's disease, there have been strong interests in differentiating human pluripotent stem cells (hPSCs) to A9 dopaminergic neurons for disease modeling and transplantation studies. Directed differentiation of hPSCs based on the development of mouse midbrain DA neurons is currently the most successful approach [11]. Human embryonic stem cells (hESCs) can be differentiated to neuroprogenitors at a very high efficiency with dual SMAD inhibitors, such as SB431542 and noggin [12]. As midbrain DA neurons are derived from radial glial cells in the midbrain floor plate (mFP) [13, 14], neuroprogenitors are regionally specified by appropriate levels of SHH (for dorsal-ventral axis [15]) and WNT1 (for rostral-caudal axis [16]). A high concentration of SHH is crucial for making ventral progenitors [17], while an intermediate level of the GSK3 inhibitor CHIR99021 (around 1 µM) activates WNT signaling to a degree that restricts neuroprogenitors to a midbrain fate [18]. The correctly specified mFP cells are terminally differentiated to dopaminergic neurons in the presence of neurotrophic factors, such as BDNF, GDNF and TGFβ3, all of which facilitate the expression of the gene battery that defines mature DA neurons [19]. Inhibition of the Notch pathway generally suppresses the differentiation of neural stem cells to glial lineages and favors neuronal differentiation [20]. Thus, the Notch inhibitor DAPT has been used in the differentiation of mESCs [21] and hPSCs [22] to neurons. Increasing intracellular cAMP concentration promotes neuronal maturation [22, 23] by enhancing the expression of voltage-dependent Na^+, K^+ and Ca^{2+} channels, which increases action potential firing and promotes Ca^{2+} signaling events critical for dendritic outgrowth and synapse formation [24].

Previously established floor plate-based protocols [18, 22, 25] work well for the differentiation of hESCs to midbrain DA neurons. When we used them to differentiate human induced pluripotent stem cells (iPSCs), we generated significantly fewer midbrain DA neurons. This is in agreement with a previous study [26] that suggests the retention of epigenetic memory in iPSCs in comparison to hESCs [27–29]. Consistent with this, two independent groups have sought to optimize a well-recognized method [18] by using an appropriate seeding pattern [30, 31] or by sorting CORIN[+] neural progenitors to enrich TH^{+} neurons [32, 33]. The most recent optimization [34] of this widely-used floor plate-based method [18] shows continuing improvements in the development of methods to differentiate hPSCs to midbrain DA neurons.

Here, we developed an enhanced method to differentiate human iPSCs to A9 dopaminergic neurons by increasing and prolonging the activation of Sonic Hedgehog signaling with purmorphamine (PM) to elevate the expression of mFP genes to similar levels as induced in hESCs. A previous study has shown

---

[1]Department of Physiology and Biophysics, State University of New York at Buffalo, Buffalo, NY 14203, USA. [2]Veterans Affairs Western New York Healthcare System, Buffalo, NY 14215, USA. [3]These authors contributed equally: Hong Li, Houbo Jiang. ✉email: jianfeng@buffalo.edu

2

that the BMP/SMAD signaling pathway plays an essential role in the development of midbrain DA neurons [35]. We found that a shorter duration of dual SMAD inhibition greatly elevated the induction of many critical genes specifying mFP and A9 DA neurons without affecting the differentiation of iPSCs or hESCs to neuroprogenitor cells. While FGF8b did not significantly affect the differentiation of mFP DA progenitors to mature A9 DA neurons, it could be used to expand mFP progenitors in vitro. The combination of these improvements enabled the differentiation of human iPSCs to A9 DA neurons that expressed appropriate markers, exhibited autonomous pacemaking and supported excellent engraftment and functional recovery in the 6-OHDA rat model of dopaminergic lesions.

MATERIALS AND METHODS
Differentiation of hPSCs to midbrain floor plate progenitors
H9 hESCs (at passages 35–45) were purchased from WiCell. The C001, C002 [36] and C005 [37] human iPSCs (at passages 25–45) were generated and cultured as described previously. Colonies of hPSCs were detached with dispase to generate embryoid bodies (EBs), which were cultured in suspension in a 1:1 mixture of DMEM/F12 and Neurobasal media with N2 Supplements (1:100), B27 supplements without vitamin A (1:50), ascorbic acid (0.2 mM), SB431542 (10 μM, Tocris), dorsomorphin dihydrochloride (DM, 5 μM, Stemgent), and various concentrations of purmorphamine (Stemgent) and CHIR99021 (CHIR, Stemgent) as indicated in each figure. On day 4, the flask containing EBs was put in a vertical position for 10 min to allow EBs to sediment. The EBs were washed with DMEM/F12 once, and then plated on the matrigel-coated plates evenly. On day 6 or day 9, SB and DM were discontinued in the medium in different experiments.

Differentiation of midbrain floor plate progenitors to A9 DA neurons
On day 16, properly specified midbrain floor plate progenitors were washed with DMEM/F12 once and dissociated to single cells with accutase at 37 °C for 5–10 min. Cells were centrifuged at $200 \times g$ for 5 min and washed with DMEM/F12 twice, and then plated onto polyornithine/matrigel-coated plates at a density of 5000–10,000 cells/cm^2 in a 1:1 mixture of DMEM/F12 and Neurobasal that contained N2, B27 without vitamin A (1:50), ascorbic acid (0.2 mM), purmorphamine (1 μM), and CHIR99021 (0.8 μM). On day 18, the medium was changed to Neurobasal with N2, B27 without vitamin A, Brain-derived Neurotrophic Factor (BDNF) (20 ng/ml), Glial cell line-derived Neurotrophic Factor (GDNF) (20 ng/ml), and TGFβ3 (1 ng/ml). On day 20, dibutyryl-cAMP (dcAMP) (0.5 mM) and DAPT (1 μM) were added to the medium. The ROCK inhibitor Y27632 (10 μM) was added during the first 48 h. Purmorphamine and CHIR99021 were gradually removed as shown in Fig. S4A. At day 24, cells were cultured in the differentiation medium without purmorphamine and CHIR99021.

Electrophysiological recordings
Whole-cell patch-clamp recordings were performed in iPSC-derived neurons at day 70 or later. Cells were perfused in artificial cerebrospinal fluid (ACSF), consisted of (in mM): 127 NaCl, 1.2 KH$_2$PO$_4$, 1.9 KCl, 26 NaHCO$_3$, 2.2 CaCl$_2$, 1.4 MgSO$_4$, 10 glucose, 290 mOsm, and 95% O$_2$/5% CO$_2$. Voltage-dependent sodium and potassium currents were recorded with the internal solution containing (in mM): 125 K-gluconate, 10 KCl, 10 HEPES, 0.5 EGTA, 3 Na$_2$ATP, 0.5 Na$_2$GTP and 12 phosphocreatine, pH 7.4, 300 mOsm. Voltage steps from -100 mV to $+40$ mV lasting 500 ms were used. For the recording of evoked action potentials, steps of currents from -60 pA to $+140$ pA lasting 1.8 s were injected into the cell. To record spontaneous action potentials, cells were held in the current-clamp mode with no current injection. Recordings of voltage-dependent Ca^{2+} currents (VDCC) used the internal solution consisting of (in mM): 170 N-methyl-D-glucamine, 40 HEPES, 4 MgCl$_2$, 5 1,2 bis-(o-aminophenoxy)-ethane-N,N,N*, N*-tetraaceticacid, 12 phospho-creatine, 3 Na$_2$ATP, 0.5 Na$_3$GTP, and 0.1 leupeptin, pH 7.2–7.3, 265–270 mosM/l. The external solution consisted of (in mM): 127 NaCl, 20 CsCl, 1 MgCl$_2$, 10 HEPES, 0.001 tetrodotoxin, 5 BaCl$_2$, and 10 glucose, pH 7.3, 300–305 mOsm. VDCC were evoked by a ramp voltage protocol from -80 mV to $+60$ mV. An Olympus BX51WI microscope was used to visualize neurons. A MultiClamp 700B amplifier (Molecular Devices, Sunnyvale, CA) was used to perform patch-clamp recordings. Signals were filtered at 4 kHz and sampled at 100 kHz using a

Digidata 1322 A analog-digital converter (Axon instruments). Data were analyzed with pClamp 10.0 (Axon Instruments) and were presented as mean ± SEM. Data points that vary by more than 3 standard deviations below or above the mean were excluded.

Animal surgery
The care and use of rats were approved by the Institutional Animal Care and Use Committee (IACUC) in the State University of New York at Buffalo. Male athymic rats (Hsd:RH-Foxn1^{rnu}, Envigo) at 8–10 weeks of age, weighing 200–250 g, were used in 6-OHDA lesion experiments. Only male athymic rats were used to maintain consistency with our previous experiments on male Sprague Dawley (SD) rats, as female SD rats did not tolerate daily cyclosporin injections. Future experiments using both sexes of athymic rats will reveal whether there are significant sex differences in response to engraftment. We injected 3 μl of 6-OHDA (5 mg/ml freebase in a solution of 0.2 mg/ml L-Ascorbic acid in 0.9% sodium chloride) using a 10 μl Hamilton syringe and a Kopf stereotaxic frame into the medial forebrain bundle (AP: -4.4; ML: -1.2; DV: -7.8) on the right hemisphere of the rat brain [38]. Four weeks later, successfully lesioned rats with more than 6 rotations/min after an apomorphine IP injection at 0.05 mg/kg body weight were used for transplantation. We randomly picked 4 rats for the sham group and the other 6 rats were used for the graft group. The A9 DA neurons at day 37 of differentiation were washed with PBS once, treated with Accutase for 5–10 min at 37 °C in an incubator. The cells were aspirated gently with a 1 ml pippet and washed twice with Neurobasal medium containing $1 \times$ B27 before they were resuspended at 37,500 cells/μl in the same medium. The cell suspension was placed in ice for no more than 1 h before transplantation. Cells were transplanted in 4 μl (37,500 cells/μl) using stereotaxic injection into the rat striatum (from the bregma: AP: $+0.5$ mm; ML: -3.0 mm; DV: -6.0 mm and -5.0 mm), with 2 μl at each location for 5 min. Fourteen weeks after transplantation, rat brains were harvested by transcardiac perfusion with paraformaldehyde (4% in PBS). Coronal sections (20 μm thick) were immunostained with the antibodies indicated.

Locomotor tests
Apomorphine-induced rotations and rotarod were performed at 0, 4, 8 and 12 weeks after cell transplantation. Rats were injected i.p. with apomorphine (0.05 mg/kg, dissolved in 0.9% NaCl containing 0.1% ascorbic acid). The number of rotations was recorded for 20 min starting 10 min after injection. The data were presented as the average number of rotations per minute. For the rotarod test, rats were pre-trained on an automated 4-lane rotarod unit (SDI Rotor-Rod, San Diego Instruments, INC, USA) that could be set on fixed speed. Then, animals were tested three times at 12 rpm with 20-minute rests between each trial. Latency to fall recorded by the rotarod device was averaged for each animal.

Quantification and statistical analysis
SPSS 13.0 was used for statistical analysis. All data are expressed as mean ± standard error of measurement. The sample sizes for animal behavior testing were estimated based on a similar experiment in a previous study [22] at $n = 4$ at least for achieving power over 0.8. Experiments with two groups were compared by unpaired, two-sided t test, where data were assessed to be normally distributed (Shapiro–Wilk test, $p > 0.05$) and equally dispersed (Levene's test, $p > 0.05$). Experiments with multiple measures for two groups were analyzed by two-way repeated measure ANOVA with Geisser-Greenhouse correction, followed by Bonferroni correction for multiple comparison. Values of $p < 0.05$ were considered statistically significant.

RESULTS
Differential efficiencies of a floor plate-based method in the differentiation of hESCs and human iPSCs to midbrain DA neurons
After testing several protocols for the differentiation of hESCs to midbrain DA neurons [18, 22, 39], we chose the one that starts with embryoid bodies (EBs) [22]. This approach avoids substantial cell death at the beginning of differentiation [30, 31] or the need to sort CORIN$^+$ cells [32, 33] when differentiation is initiated in hPSC colonies grown on matrigel [18]. When we differentiated H9 hESCs with the Kirkeby method [22] (Fig. 1A), 69.1 ± 10.1% of
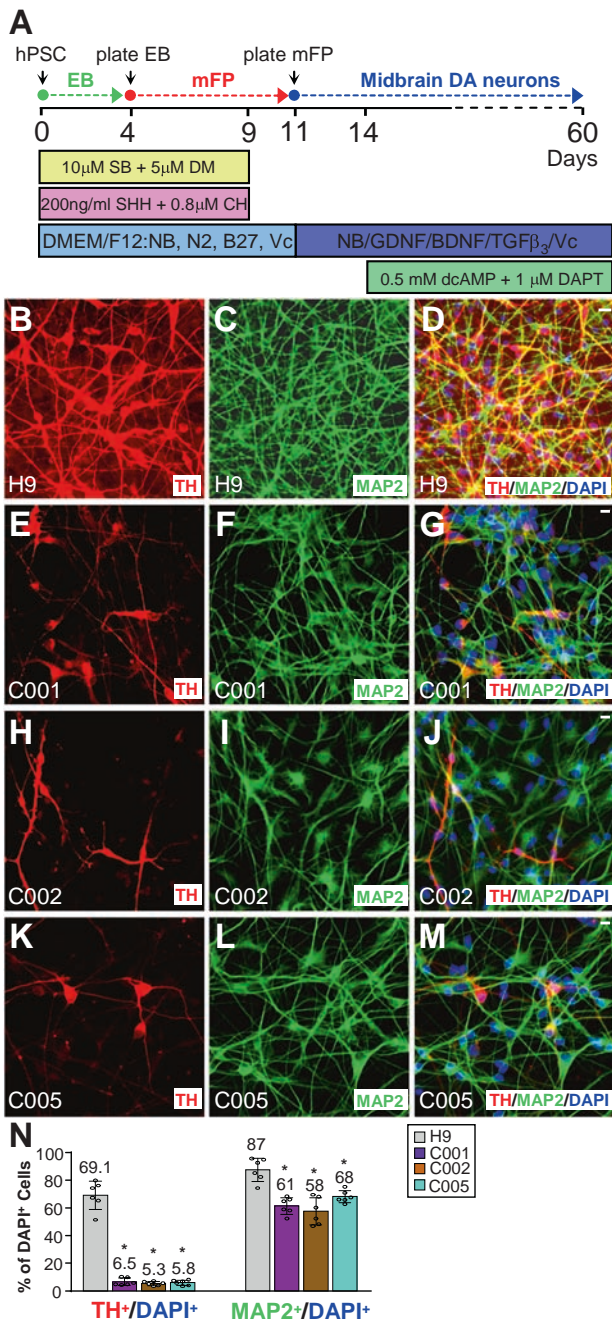
Fig. 1 An existing floor plate-based protocol has different efficacies in differentiating human iPSCs and hESCs to midbrain DA neurons. A Using the Kirkeby method [22], we differentiated human pluripotent stem cells (hPSCs) in suspension culture to embryoid bodies (EBs), which were replated and differentiated to midbrain floor plate (mFP) progenitors and then to midbrain DA neurons. Concentrations of medium components are in the methods section. **B–M** Immunostaining for TH (**B, E, H, K**), MAP2 (**C, F, I, L**), together with DAPI (**D, G, J, M**) of neurons differentiated from H9 hESCs (**B–D**), C001 (**E–G**), C002 (**H–J**) or C005 (**K–M**) human iPSCs. Bars, 10 μm, for the whole row where absent. **N** Percentages of TH+ or MAP2+ neurons in cells differentiated from H9 hESCs or C001, C002 and C005 human iPSCs. *$p < 0.05$, unpaired t test, vs. H9, $n = 6$ from 3 independent experiments with 2 wells for each experiment.

DAPI+ cells were TH+ neurons (Fig. 1B–D, N). When we used the same method to differentiate three independent lines of normal human iPSCs, only 5–6% of DAPI+ cells were TH+ neurons (Fig. 1E–N), regardless of whether the human iPSCs were

generated with integrating lentiviruses (C001 and C002 iPSCs) [36] or with non-integrating episomal plasmids (C005) [37]. The generation of MAP2+ mature neurons was not affected as markedly (Fig. 1N). Pluripotency makers, such as NANOG, SOX2, SSEA3, and OCT4, were expressed at indistinguishable levels in these iPSCs and H9 hESCs (Fig. S1A–E). Information on antibodies, chemicals, and growth factors is listed in Supplementary Table S1.

Improving the differentiation of human iPSCs to midbrain floor plate DA progenitors

We optimized the activation of the Sonic Hedgehog (SHH) signaling pathway to specify floor plate cells [17] and the activation of the WNT pathway to acquire a midbrain fate [40]. First, we used various concentrations of purmorphamine (PM), a small-molecule activator of SHH signaling [41, 42], to treat C002 iPSCs or H9 hESCs for 9 days, in a medium containing the dual SMAD inhibitors SB431542 (10 μM) and dorsomorphin (5 μM) (Fig. 2A). As a robust induction of floor plate genes, such as FOXA2 and CORIN, is seen around day 14 in a previous study [18], we performed qRT-PCR to measure the expression of various marker genes at day 14. Sequences of PCR primers are listed in Supplementary Table S2. In cells differentiated from C002 iPSCs, expression of the floor plate markers FOXA2 and CORIN, as well as the midbrain markers LMX1A and LMX1B, peaked at 3 μM PM. In contrast, the forebrain marker PAX6 decreased dramatically in the presence of PM, and the hindbrain marker HOXA2 increased substantially at PM of 3 μM or above (Fig. 2C). On the other hand, cells differentiated from H9 hESCs showed peak expression of FOXA2 and LMX1B at 1 μM PM and increasing expression of CORIN and LMX1A with PM. PAX6 expression was abolished by PM, while HOXA2 increased dramatically at PM of 2 μM or above (Fig. 2D). We confirmed these results with immunostaining of cells differentiated from C002 iPSCs (Fig. 2E) or H9 hESCs (Fig. 2F). Thus, the optimal PM concentration for C002 iPSCs was 3 μM, in contrast to 1 μM for H9 hESCs. At such concentrations of PM, expression of critical marker genes had significant differences compared to those induced by the lower or the higher concentration.

Using these concentrations for PM, we then optimized the concentration of CHIR99021 (CH), a potent GSK3 inhibitor that activates WNT signaling to mimic rostral-caudal specification [25], in the differentiation of C002 iPSCs and H9 hESCs to generate a midbrain cell fate (Fig. 2B). Increasing doses of CH (0, 0.4, 0.8, 1.6 μM) were added to the medium containing SB431542 (10 μM) and dorsomorphin (5 μM), in addition to 3 μM PM for C002 iPSCs or 1 μM PM for H9 hESCs for 9 days (Fig. 2B). The expression of CORIN was not significantly affected by CH in both C002 (Fig. 2G) and H9 (Fig. 2H), while the expression of FOXA2, LMX1A and LMX1B increased with CH concentrations (Fig. 2G, H). The expression of OTX2 and SOX6, markers of midbrain dopaminergic progenitors, peaked at 0.8 μM of CH in both C002 (Fig. 2G) and H9 (Fig. 2H). However, the expression of the hindbrain marker HOX2 elevated dramatically when CH concentration was greater than 0.8 μM for both C002 (Fig. 2G) and H9 (Fig. 2H). When CH was at 0.8 μM, the expression of critical marker genes had significant differences compared to those induced by the lower or the higher concentration. These qRT-PCR results were confirmed by immunostaining (Fig. 2I, J). Thus, the optimal concentration for CH was 0.8 μM for both C002 and H9, along with 3 μM PM for C002 or 1 μM PM for H9.

We compared the efficacies of PM and SHH by differentiating C002 iPSCs in medium containing SB431542 (10 μM), dorsomorphin (5 μM), CH (0.8 μM) and SHH at 200 ng/ml or 500 ng/ml or PM at 3 μM for 9 days. PM at 3 μM induced the highest expression of FOXA2 (Fig. S1F) and CORIN (Fig. S1G), lowest expression of PAX6 (Fig. S1H), and unchanged expression of HOXA2 (Fig. S1I). Adding 200 or 500 ng/ml SHH to 3 μM PM achieved no further effects (Fig. S1F–I). Thus, PM can replace SHH in the differentiation of iPSCs.
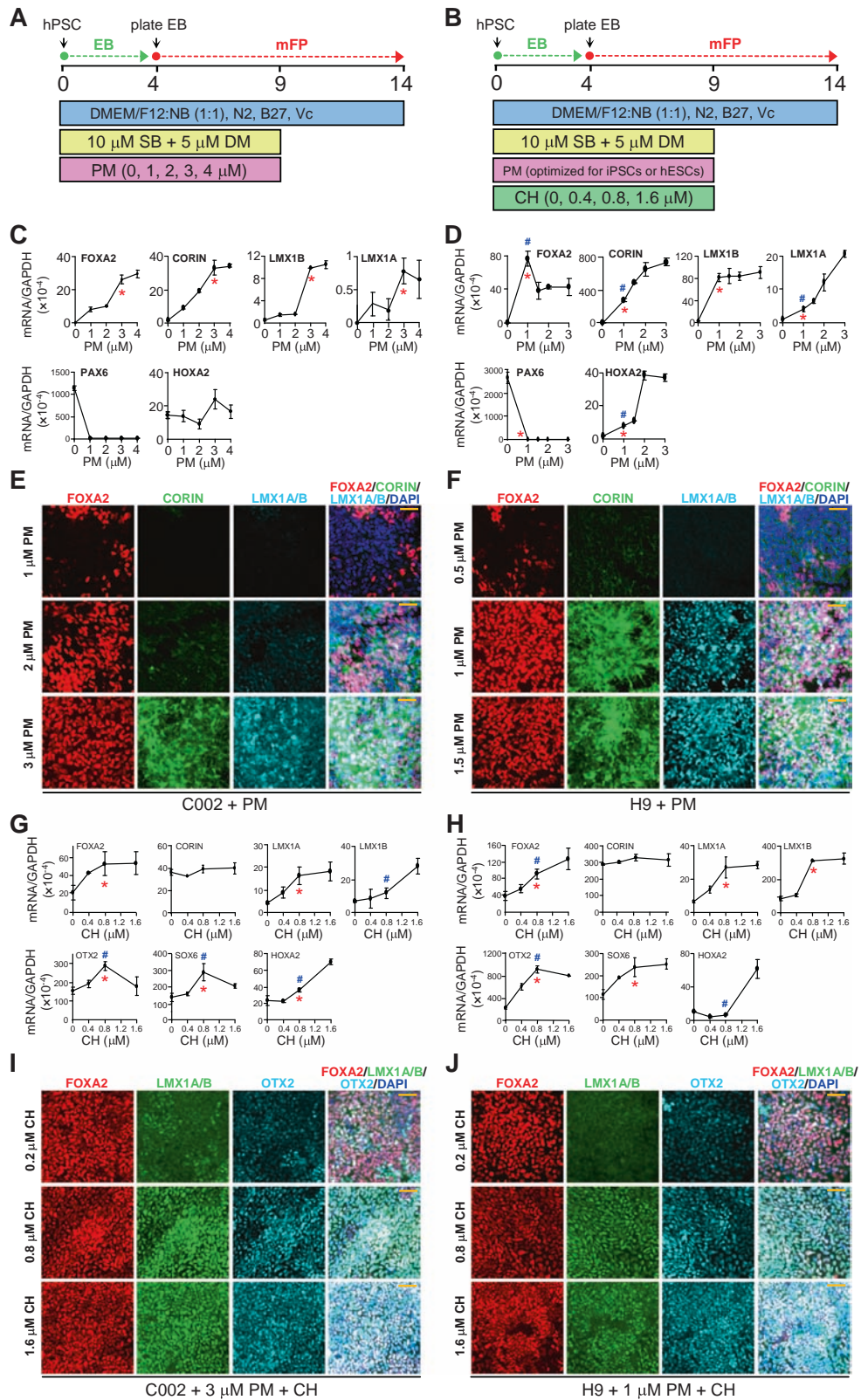
Shortening dual SMAD inhibition facilitates dopaminergic differentiation

Previous methods for the differentiation of hPSCs to midbrain DA neurons use the dual SMAD inhibitors dorsomorphin (5 μM) and SB431542 (10 μM) or noggin for 9 days at the beginning of differentiation [18, 22, 39]. We found that in such regimens, the expression of OCT4 and NANOG were rapidly abolished within the first two days, while the induction of the neural stem cell markers SOX1 and NESTIN plateaued around day 4 (Fig. 3A). As BMP/SMAD signaling is critical in the development of midbrain DA neurons

Fig. 2 Optimizing the differentiation of human iPSCs to floor plate DA progenitors. A Concentrations of purmorphamine (PM) were optimized for the differentiation of human pluripotent stem cells (hPSCs) in the indicated base medium with SB431542 (10 μM) and dorsomorphin (5 μM) for 9 days and maintained in the base medium to day 14. **B** After the optimal PM concentration was identified for the differentiation of human iPSCs or hESCs, the schematic was used to optimize the concentration of CHIR99021 (CH). **C**–**F** C002 human iPSCs (**C**, **E**) or H9 hESCs (**D**, **F**) were differentiated as in schematic (**A**). Expression of indicated marker genes was analyzed by qRT-PCR (**C**, **D**) and immunostaining (**E**, **F**) at day 14. **G**–**J** C002 (**G**, **I**) or H9 (**H**, **J**) were differentiated with 3 μM or 1 μM PM, respectively, and varying concentrations of CHIR99021 (CH) as in schematic (**B**). Expression of indicated genes was examined by qRT-PCR (**G**, **H**) and immunostaining (**I**, **J**) at day 14. $n =$ 6 from 3 independent experiments, with 2 wells for each experiment. $*p < 0.05$, vs. the lower concentration; $\#p < 0.05$, vs. the higher concentration, all unpaired t test. Bars, 100 μm.

◀

[35], we tested whether shortening dual SMAD inhibition might enhance the differentiation of iPSCs to midbrain DA neurons. When we changed dual SMAD inhibition from the first 9 days to the first 6 days, there were no significant differences in the percentages of SOX1+ cells, NESTIN+ cells, or SOX1+NESTIN+ cells among all cells at day 14 (Fig. 3B–D). However, expression levels of LMX1B, SOX6, PITX3, ASCL1, MSX1 and MSX2 were significantly increased at day 14 (Fig. 3E, F). Further differentiation of these mFP cells to DA neurons at day 32 revealed significant increases in the expression levels of TH, ALDH1A1, PITX3, GIRK2, and EN1 (Fig. 3G, H).

Prolonged ventral midbrain specification improves marker gene expression

Using the optimized differentiation protocol (Fig. 4A), we examined the expression of various marker genes when PM and CH were used for up to 16 days. As expected, NANOG and OCT4 expression ceased within two days (Fig. 4B). Expression of floor plate genes FOXA2 and CORIN was substantially elevated at day 16 than at day 8, as was the expression of the endogenous ventralization factor SHH (Fig. 4B). Expression of midbrain dopaminergic markers, such as LMX1A, LMX1B and PITX3, was markedly increased at day 16 than at day 8, while the levels of OTX2 and SOX6 were similar at the two time points (Fig. 4C). We confirmed the qRT-PCR results by costaining cells at day 16 for FOXA2, LMX1A/B, OTX2 and DAPI (Fig. 4D), as well as CORIN, SOX6, FOXA2 and DAPI (Fig. 4E). The percentages of each of these markers in all DAPI+ cells were over 94% (Fig. 4F).

Previous studies have shown that in the presence of GSK3β inhibitors, FGF8b had only marginal effects [18] or was not necessary [22, 39] in the differentiation of hPSCs to midbrain DA neurons. We differentiated C002 iPSCs to mFP progenitors using the protocol in Fig. 4A in three different scenarios: (1) no FGF8b throughout; (2) with FGF8b (100 ng/ml) for days 0–8; (3) with FGF8b (100 ng/ml) for days 8–16. Further differentiation of these three kinds of mFP progenitors to midbrain DA neurons showed no significant difference in the percentages of TH+ neurons among all DAPI+ cells at day 60 (Fig. S2A–D). We found that mFP progenitors did not proliferate in basal media (B) or basal media plus PM and CH (BPC) but expanded substantially in media with FGF8b (BPCF) (Fig. S2E, F). EdU incorporation assays [43] showed that FGF8b significantly increased the percentage of EdU+ cells (Fig. S2G–J). Unpassaged mFP progenitors generated in BPC medium without FGF8b expressed CORIN, LMX1A/B, and FOXA2 (Fig. S2K). In the presence of FGF8b, expression of CORIN, LMX1A/B and FOX2 were maintained in cells with a generally similar round morphology from passages 1 to 3 (Fig. S2N, O, Q); expression of OTX2 and EN1 was maintained as well (Fig. S2P, R). In basal media (B) without PM and CH, FOXA2 and LMX1A/B expression was lost with the concomitant change of cellular morphology (Fig. S2L). At passage 1, neuronal processes started to extend from mFP progenitors still positive for CORIN, LMX1A/B and FOXA2, when FGF8b was not present (Fig. S2M). The addition of FGF8b restored the generally round morphology of mFP progenitors (Fig. S2N). Together, these data indicate that FGF8b is not necessary for the differentiation of mFP progenitors to midbrain DA neurons but can be used to expand mFP progenitors.

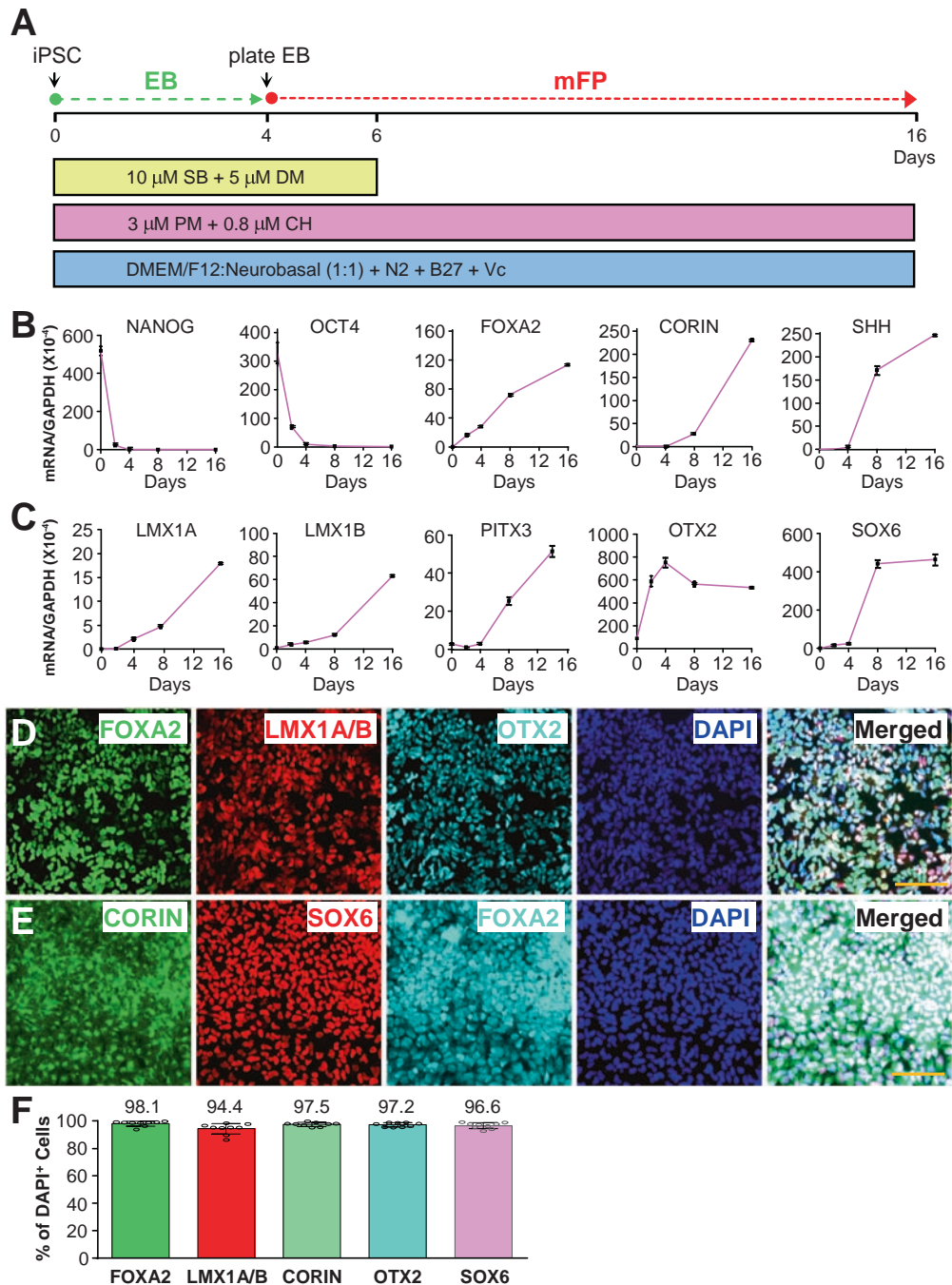### Differentiation of mFP progenitors to midbrain DA neurons expressing A9 markers

To induce the terminal differentiation of midbrain floor plate (mFP) progenitors to midbrain DA neurons, we gradually reduced PM to 1 μM from days 16–24 and removed CH at day 20. The base medium was changed from a 1:1 mixture of DMEM/F12 and Neurobasal to 100% Neurobasal containing N2 and B27 supplements and vitamin C, as well as dcAMP (0.5 mM) [22, 23], DAPT (1 μM) [22], GDNF (20 ng/ml), BDNF (20 ng/ml), and TGFβ3 (1 ng/ml) [18, 22, 39], which are all important for the terminal differentiation of midbrain DA neurons (Fig. 5A). At day 60, neurons with complex morphology and extensive processes (Fig. 5B) were immunostained for TH, Tuj1 or MAP2. We found that 72.5 ± 14.3% of all DAPI+ cells were TH+ neurons, 98.0 ± 3.8% of all cells were Tuj1+ neurons, and 95.7 ± 4.1% of all cells were MAP2+ mature neurons (Fig. 5C–I). We also costained the neuronal cultures for TH and the floor plate markers CORIN (Fig. 5J) and FOXA2 (Fig. 5K), midbrain markers EN1 (Engrailed 1) (Fig. 5L) and NURR1 (Fig. 5M), A9 DA neuron markers ALDH1A1 (Fig. 5N) and GIRK2 (Fig. 5O), as well as the A10 marker CALBINDIN (Fig. 5P). Except for CALBINDIN, which was expressed in only 7.5 ± 2.1% TH+ neurons, all the other markers were expressed in at least 82% of TH+ neurons (Fig. 5Q). Thus, the majority of these midbrain DA neurons expressed markers for A9, but not A10 DA neurons. Separate channels of Fig. 5J–P are shown in Fig. S3. Using the same method, we differentiated C001 and C005 iPSCs and H9 hESCs to midbrain DA neurons. There were no significant differences in the percentages of TH+ neurons, Tuj1+ neurons or MAP2+ neurons in all DAPI+ cells among the four lines (Fig. S4). Both C001 and C002 iPSCs are generated with integrating lentiviruses [36], while C005 iPSCs are generated with non-integrating episomal plasmids [37].

iPSC-derived neurons exhibit the autonomous pacemaking property of A9 DA neurons

Whole-cell patch-clamp recordings [36] of C002 iPSC-derived neurons at day 70 showed that they had voltage-dependent Na+ (inward) and K+ (outward) currents in response to voltage steps (Fig. 6A and enlarged inset). Most neurons at days 40–59, and almost all neurons at day 60 or later had these currents. We found significantly increased peak currents and corresponding changes in the I–V curves of voltage-gated Na+ and K+ currents as the neurons became more mature from days 40 to 120 (Fig. S5A–H). Almost all neurons at day 60 or later had evoked action potentials in response to injected currents (Fig. 6B). In DA neurons at days 80-120, spontaneous action potentials (sAP) were observed (Fig. 6C). The sAP was not significantly affected by the AMPA and kainate receptor blocker DNQX (Fig. 6D) or the NMDA receptor blocker AP5 (Fig. 6E) but was abolished by the L-type Ca^{2+} channel blocker nimodipine (Nim) (Fig. 6F) or the Na+ channel blocker TTX (Fig. 6G). Statistical analysis of the results is shown in Fig. 6H. These data indicate that the spontaneous action potentials are autonomous pacemaking activities independent of glutamatergic input but dependent on L-type Ca^{2+} channels, like the pacemaking properties of A9 DA neurons in rat brains [44]. Analysis of sAP in 703 traces from 16 neurons showed that these APs shared remarkable similarities to those recorded from nigral
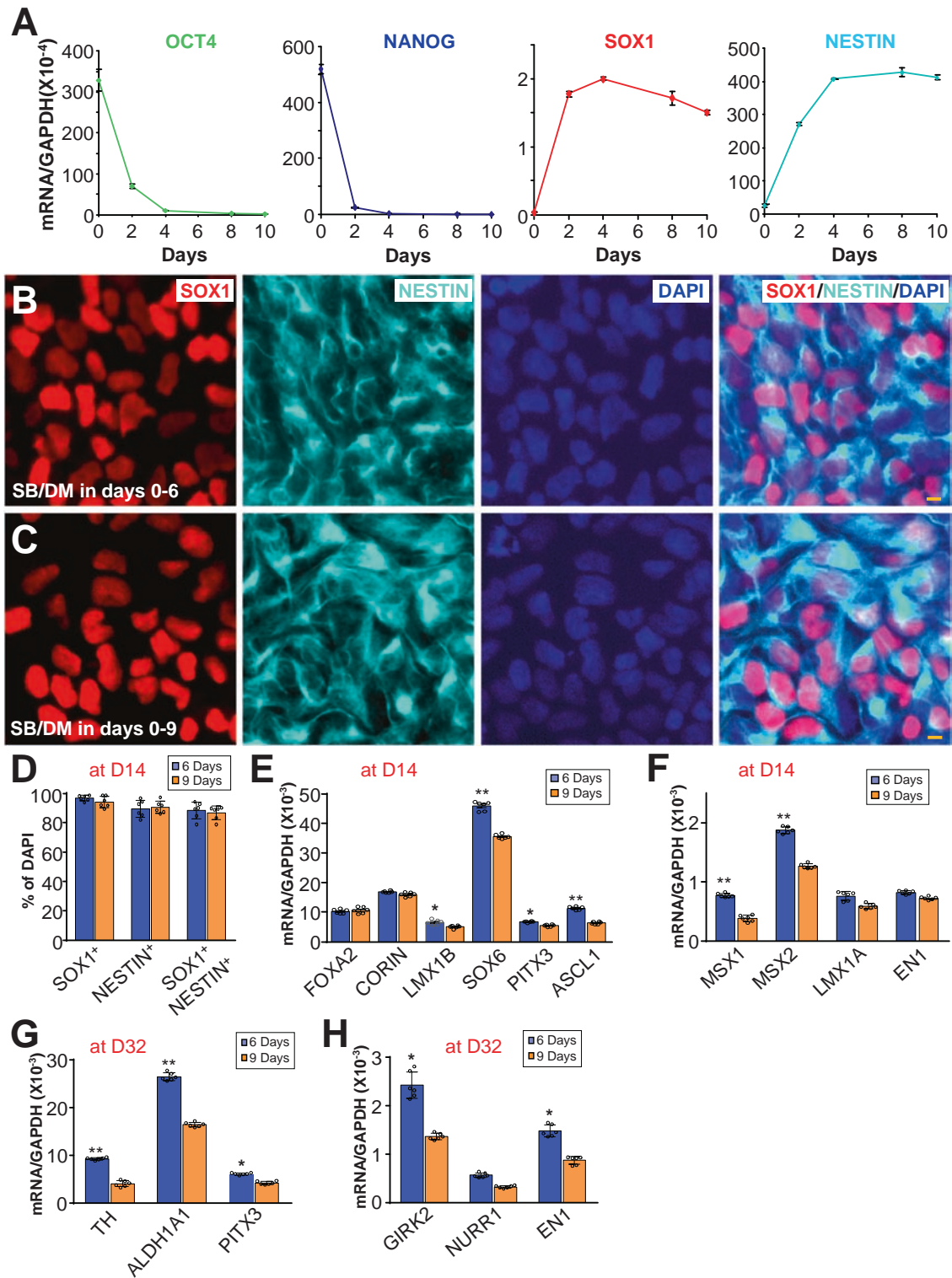
Fig. 3 Optimal timing of dual SMAD inhibitors for the generation of midbrain DA neurons. A Expression levels of the indicated genes at various time points during the differentiation of C002 iPSCs in DMEM/F12:Neurobasal (1:1) with N2/B27 (without vitamin A), ascorbic acid (0.2 mM), purmorphamine (3 µM), CHIR99021 (0.8 µM), SB431542 (SB, 10 µM) and dorsomorphin (DM, 5 µM) for 9 days. **B–F** SB and DM were withdrawn at day 6 (**B**) or day 9 (**C**) during differentiation. Bars, 10 µm. Cells were stained as indicated at day 14 and quantified (**D**). Expression of the indicated midbrain floor plate marker genes was measured at day 14 (**E**, **F**). **G, H** Expression of the indicated dopaminergic marker genes was measured at day 32 after differentiation of midbrain floor plate progenitor cells to DA neurons. $*p < 0.05$, $**p < 0.01$, unpaired t test, 6 days vs. 9 days, $n = 6$ from 3 independent experiments, with 2 wells for each experiment.
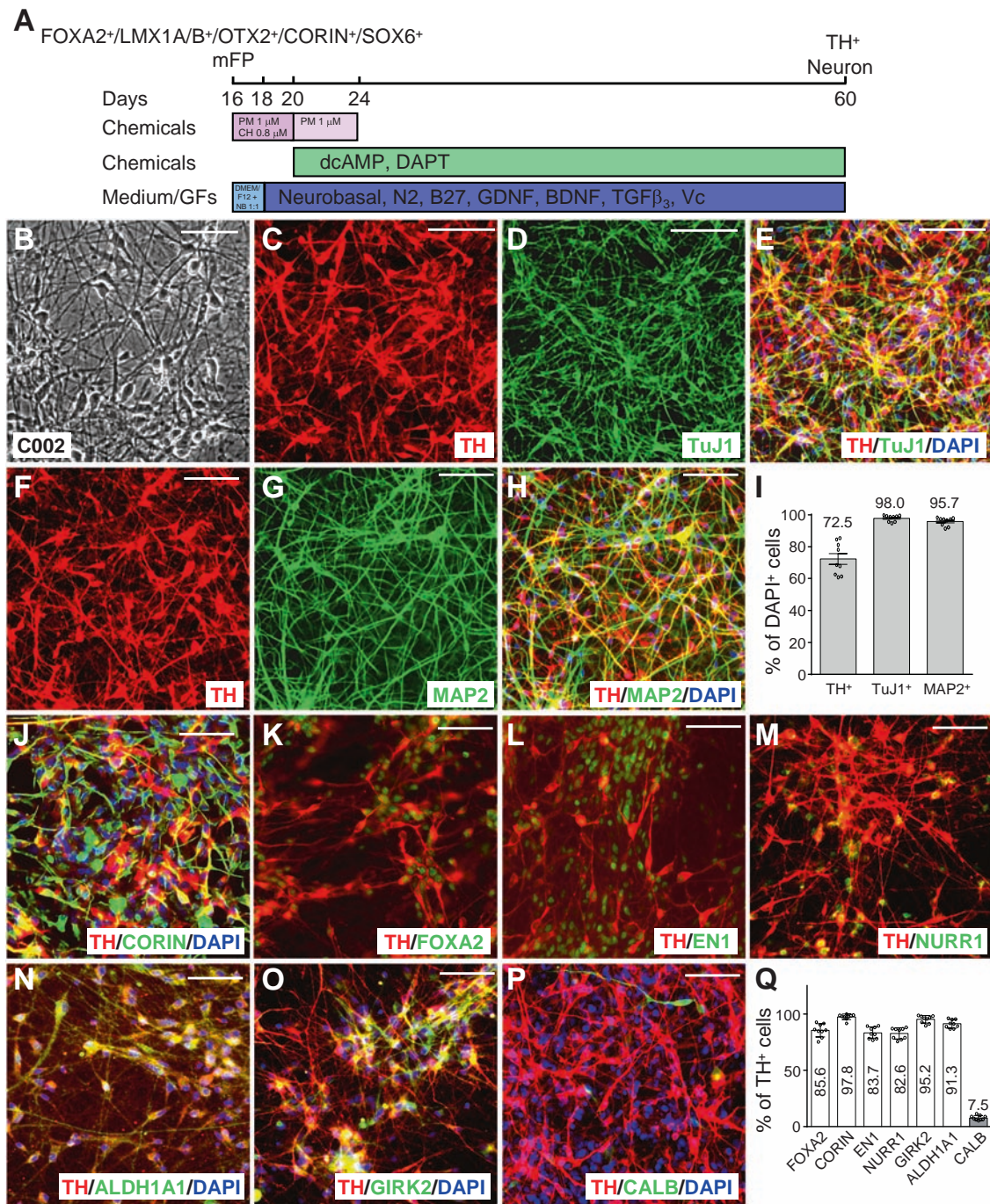
Fig. 4 Generation of midbrain floor plate DA progenitors from human iPSCs using small-molecule compounds. A The optimized protocol for the differentiation of human iPSCs to midbrain floor plate (mFP) DA progenitors through embryoid bodies (EB). SB SB431542, DM Dorsomorphin, PM purmorphamine, CH CHIR99021. **B, C** qRT-PCR measurements of the expression of the indicated genes at different days of differentiation. **D–F** Immunostaining for the indicated markers at day 16 of differentiation (**D, E**) was quantified in (**F**). $n = 9$ from 3 independent experiments, with 3 wells for each experiment. Bars, 100 μm.

DA neurons in rat brain slices [45], with slow firing rate (5.03 ± 0.60 Hz) (Fig. 6H), relatively long AP duration (4.47 ± 0.51 ms half-width), similar AP amplitude (66.36 ± 1.60 mV), and prominent hyperpolarization (Fig. S5I–K). These properties are in sharp contrast to those of the APs fired by nigral non-DA neurons, which have much higher frequencies and shorter half-width [45].

Activating the dopamine D_2 autoreceptors with quinpirole significantly decreased the frequency of spontaneous action potentials in a reversible manner (Fig. 6I, J). Consistent with this, spontaneous dopamine release as measured by HPLC [36] was

significantly reduced by quinpirole (Fig. 6K). Voltage-dependent Ca^{2+} currents, which could be largely blocked by nimodipine, were significantly decreased by quinpirole (Fig. 6L, M). Thus, quinpirole-induced reduction of Ca^{2+} currents may decrease the frequency of pacemaking action potentials, as A9 DA neurons depend on L-type Ca^{2+} channels for pacemaking [44]. We did not study the hyperpolarization-induced current (I_h), which is present in DA neurons in both the SNc [45] and the VTA [46] and thus cannot be used to distinguish A9 and A10 DA neurons. More importantly, many neurons with the I_h current are TH$^-$ [46–48].

Fig. 5   Differentiation of midbrain floor plate DA progenitors to A9 DA neurons. A–I Using the protocol in (**A**), midbrain floor plate DA progenitors derived from C002 iPSCs were differentiated to neurons (**B**), which were stained at day 60 for the indicated markers (**C–H**) and quantified (**I**). **J–P** Neurons at day 60 were stained for the indicated markers for midbrain DA neurons (**J–M**), A9 DA neurons (**N, O**) or CALBINDIN (**P**), a marker for A10 DA neurons. **Q** Percentages of TH⁺ neurons expressing the indicated markers were quantified. Bars, 100 μm. $n = 9$ from three independent experiments, with 3 wells for each experiment.

Transplantation of iPSC-derived A9 DA neurons in rat brains

We transplanted C002 iPSC-derived A9 DA neurons (150,000 cells in 4 μl at two vertical locations with 2 μl each) at day 37 of differentiation to the striatum of athymic nude rats, which were lesioned with 6-OHDA in the medial forebrain bundle on the ipsilateral side. Fourteen weeks after transplantation, a large number of human cells positive for human nuclear antigen (hNA) were found in the rat striatum (Fig. 7A). This was confirmed by DAB staining for hNA (Fig. S6A and inset). Many of these human cells were TH⁺ in immunofluorescence staining (Fig. 7A), which

was confirmed by DAB staining for TH (Fig. 7A inset and Fig. S6B). Immunofluorescence staining showed that the TH⁺ neurons transplanted in the rat striatum were also positive for human NCAM, hNA, FOXA2, LMX1A/B, EN1, NURR1 and SOX6 (Fig. 7B–H). More importantly, these human TH⁺ neurons coexpressed the A9 markers GIRK2 (Fig. 7I) and ALDH1A1 (Fig. 7J), but not the A10 marker CALBINDIN (Fig. 7K). Separate channels of these images are shown in Fig. S7. DAB staining for hNCAM showed massive neuronal processes extended by the grafted human neurons (Fig. 7L and insets). Many hNCAM⁺ neurons were TH⁺ (Fig. S6C
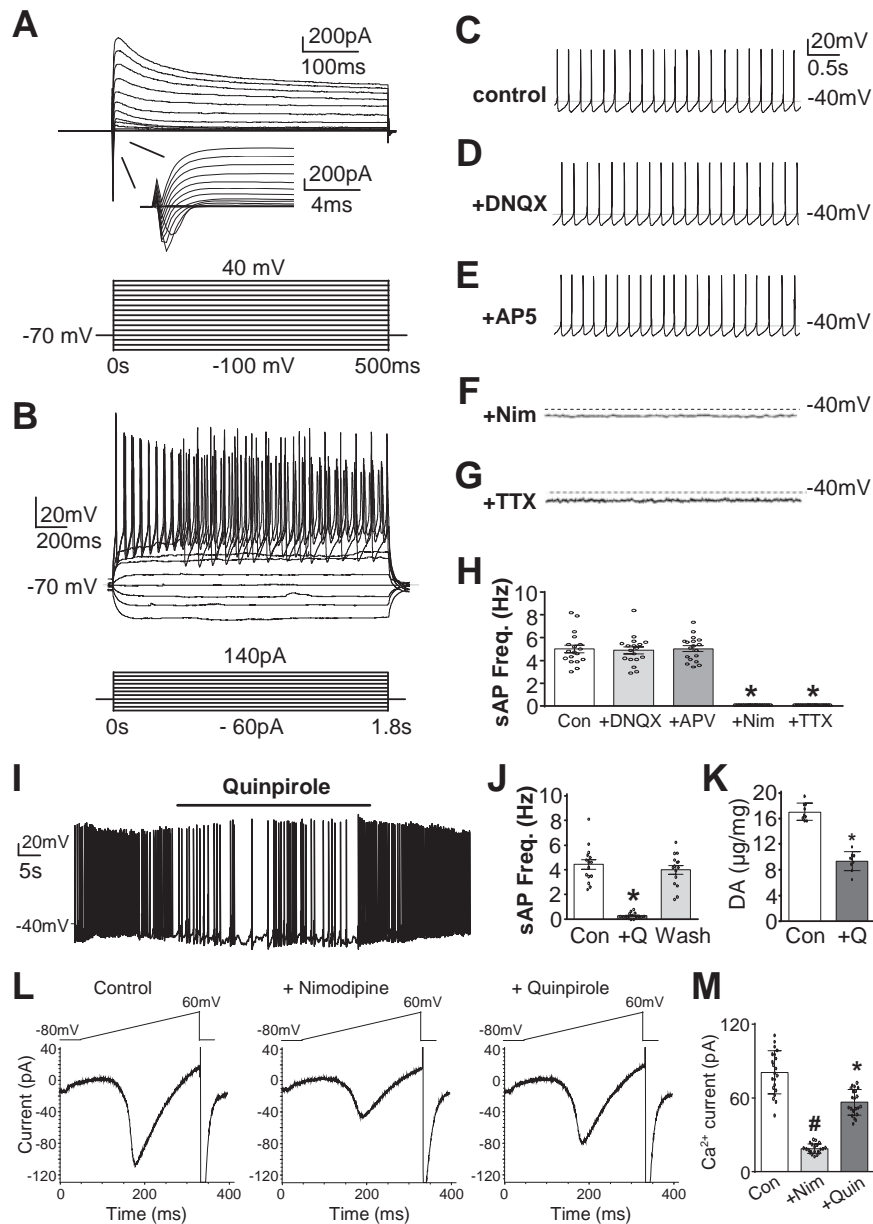
Fig. 6 Physiological properties of iPSC-derived A9 dopaminergic pacemakers. A Voltage-dependent Na$^+$ currents (inward) and K$^+$ currents (outward) in C002-derived neurons at day 70 of differentiation. **B** Evoked action potentials in response to current injections. **C**–**H** Representative traces of spontaneous action potentials (sAP) in the presence of vehicle control (**C**), 20 μM DNQX (**D**), 50 μM AP5 (**E**), 20 μM Nimodipine (Nim) (**F**), or 1 μM tetrodotoxin (TTX) (**G**), with statistical summary of sAP frequencies under the indicated conditions (**H**). *$p <$ 0.001, unpaired t test, vs. control, $n = 18$ from 4 independent experiments. **I, J** A representative trace of sAP in the absence or presence of 20 μM quinpirole (**I**), with statistical summary of sAP frequencies under the indicated conditions (**J**). *$p < 0.001$, unpaired t test, vs. control, $n = 15$ from 5 independent experiments. **K** Spontaneous dopamine release in the absence (Con) or presence of 20 μM quinpirole (Q). *$p < 0.05$, unpaired t test, vs. control, $n = 9$ from 3 independent experiments, each with 3 wells of cells. **L, M** Representative traces of voltage-dependent Ca^{2+} currents in the presence of vehicle control, 20 μM Nimodipine, or 20 μM quinpirole, with statistical summary of peak Ca^{2+} currents under the indicated conditions (**M**). *$p < 0.05$, #$p < 0.0001$, unpaired t test, vs. control, $n = 21$ from 7 independent experiments.

and Fig. 7B for enlarged view). Locomotor deficits induced by 6-OHDA lesion were gradually and significantly alleviated when we measured apomorphine-induced rotations (Fig. 7M) or latency to fall on the rotarod (Fig. 7N) in the rats at 4, 8 and 12 weeks after engraftment.

DISCUSSION
In this study, we developed an efficient method for the directed differentiation of human iPSCs to A9 DA neurons in chemically defined media. By mimicking the development of midbrain DA

neurons in vivo [11], we optimized the timing, duration and concentrations of various chemicals that properly direct the differentiation of iPSCs to midbrain floor plate (mFP) DA progenitors. Most of the current mFP-based methods initiate differentiation in hPSCs cultured on matrigel [18, 30–34]. While the approach is very effective for hESCs, its use on human iPSCs calls for various adaptations, such as optimal seeding pattern of iPSCs in the initial phase of differentiation [30, 31] or sorting of CORIN$^+$ mFP cells to boost the yield of TH$^+$ neurons [32, 33]. A recent optimization of the matrigel approach adopts phasic applications of CH in a medium without knockout serum replacement (KSR)
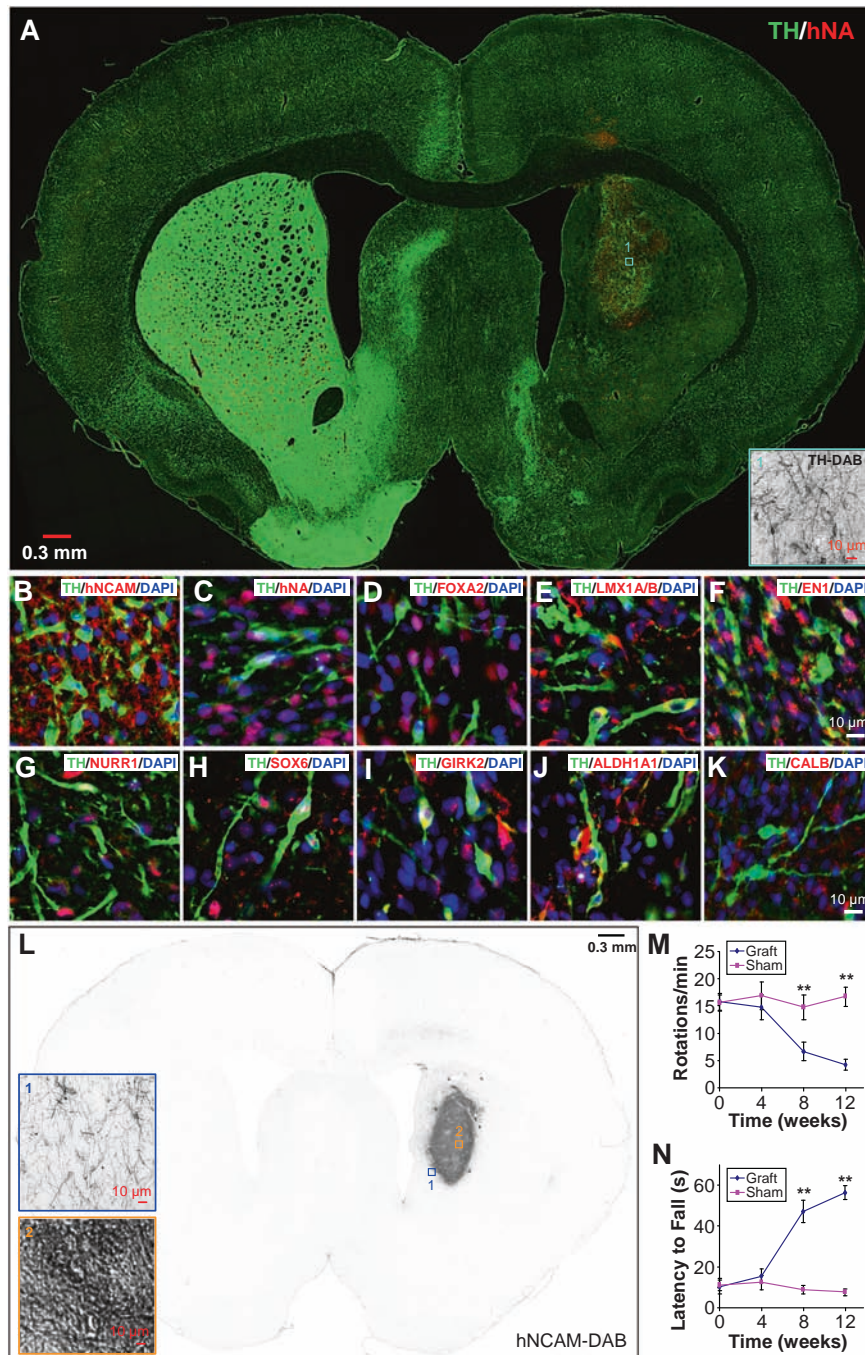
Fig. 7 Grafting iPSC-derived A9 DA neurons in rat brains. A C002 iPSC-derived A9 DA neurons (150,000 in 4 µl) at day 37 were transplanted to the striatum of 6-OHDA-lesioned athymic rats. After 14 weeks, rat brain sections were costained for TH and human nuclear antigen (hNA). Bar, 0.3 mm. Inset, anti-TH DAB staining of the boxed area in the graft (1). **B–K** Grafted neurons exhibited costaining for TH and hNCAM (**B**), TH and hNA (**C**), TH and FOXA2 (**D**), TH and LMX1A/B (**E**), TH and EN1 (**F**), TH and NURR1 (**G**), TH and SOX6 (**H**), TH and GIRK2 (**I**), TH and ALDH1A1 (**J**), but lack of costaining for TH and CALBINDIN (**K**). Bars, 10 µm. **L** Anti-hNCAM DAB staining of a coronal section with grafted human neurons. Insets, enlargement of the boxed areas. Bar, 0.3 mm. **M**, **N** Quantification of apomorphine-induced rotations (**M**) or latency to fall on rotarod (**N**) in 6-OHDA-lesioned athymic rats at the indicated time after receiving iPSC-derived neurons (graft, $n = 6$) or sham injection of the same volume of 0.9% NaCl solution (sham, $n = 4$), $**p < 0.01$, two-way repeated measure ANOVA followed by Bonferroni correction for multiple comparisons, graft vs. sham.

[34], in contrast to the original constant exposure of CH [18] in a medium with KSR, which contains lysophosphatidic acid, a substance that interferes with WNT activation by CH [49]. Because of these issues, we chose to optimize another mFP-based method that initiates the differentiation of hPSCs in embryoid bodies (EBs) in suspension culture without KSR [22]. When properly-specified EBs are attached to the plate, they produce mFP cells with distinct

morphology and clear demarcation from non-mFP cells in the periphery, which can be readily scraped away so that only mFP cells are differentiated further to neurons. This advantage is highly valuable, despite the technically more demanding requirement for making high-quality EBs.

We made several improvements to the EB-based floor plate method [22], which work very well in the differentiation of hESCs,

but not human iPSCs, to midbrain DA neurons. First, the concentration of purmorphamine needed to be substantially higher for human iPSCs (3 μM) than for hESCs (1 μM). This reflects what it may take to overcome the subtle epigenetic differences between human iPSCs and hESCs [27–29], as their differentiation to midbrain DA neurons in a rosette-based method also shows significant differences [26]. The specification of a midbrain fate was achieved using the same concentration of CHIR99021 (0.8 μM) in the differentiation of both human iPSCs and hESCs. Second, prolonged specification of ventral midbrain fate using 3 μM purmorphamine and 0.8 μM CHIR99021 for 16 days (instead of 9 days for hESCs in previous methods) was important for the differentiation of human iPSCs to midbrain floor plate (mFP) DA progenitors, as evidenced by continued increases in the expression of many important marker genes. We decreased the concentrations of purmorphamine and CHIR99021 stepwise at days 16–24, as the mFP DA progenitors were further differentiated to mature DA neurons. Third, it is important to shorten the initial dual SMAD inhibition from 9 days to 6 days, which significantly increased the expression of mFP genes at day 14 and midbrain DA markers and A9 markers at day 32. This surprising finding is consistent with the critical role of BMP/SMAD signaling in the development of midbrain DA neurons [35]. An option to expand the mFP DA progenitors is built into this protocol by passaging the progenitors in the presence of FGF8b (100 ng/ml) at least three times without substantially affecting differentiation efficiency. The caveat is that FGF8b induces the production of hindbrain cells and various types of mesenchymal-like cells [34].

The combination of these improvements generated midbrain DA neurons that expressed A9 markers such as ALDH1A1 and GIRK2, but largely not the A10 marker CALBINDIN. Most interestingly, the DA neurons exhibited autonomous pacemaking activities independent of glutamatergic input but dependent on L-type Ca^{2+} channels. These activities were very similar to what has been observed in rodent nigral DA neurons in brain slices [8, 44]. Previous studies have generated human midbrain DA neurons that fire action potentials with regularity [18, 50, 51]. The defining feature of autonomous pacemaking is that the action potentials are not significantly affected when synaptic inputs are blocked [52], as exhibited by our A9 DA neurons. L-type Ca^{2+} channel-based autonomous pacemaking is one of the unique vulnerabilities of nigral DA neurons [53], as increased demand for Ca^{2+} handling exacerbates oxidative stress contributed by dopamine catabolism [54]. Furthermore, we found that the frequency of autonomous pacemaking action potentials was significantly and reversibly reduced when the dopamine D2-class receptors were activated by quinpirole. This hallmark physiological response of nigral DA neurons serves to autoregulate dopamine release [55].

Finally, engrafted human DA neurons showed excellent survival, fiber outgrowth, expression of correct marker genes and alleviation of motor deficits. Transplantation of iPSC-derived A9 DA neurons may change other behaviors in addition to decreased apomorphine-induced rotations and improved performance on rotorod. Future studies on the full range of behavioral changes in exploration, learning, habit, etc., will reveal important functions of human nigral DA neurons grafted in the striatum of 6-OHDA-lesioned rats. Nigral DA neurons have massive axon arborization [3], whose vulnerability increases with size [56, 57]. Only midbrain DA neurons properly specified with the floor plate-based differentiation methods are able to survive in a rodent brain, generate extensive processes and reduce locomotor deficits in rodent PD models. DA neurons differentiated from hESCs using the floor plate methods show equivalency to human fetal ventral mesencephalic tissue when grafted in the rat 6-OHDA PD model [39]. Clinical trials using hESC-derived [58] or iPSC-derived [33] midbrain DA neurons differentiated with the floor plate methods [18, 32] are being conducted [59]. Continuing improvements in

the differentiation of hPSCs to midbrain DA neurons [34] will help the field better understand the properties of these cells and their vulnerability in PD. Our study showed that the human midbrain dopaminergic neurons that we differentiated from iPSCs had many important characteristics of A9 DA neurons. These results will stimulate efforts to replicate our findings and use the method to study the function and dysfunction of human A9 DA neurons. We intend to write a detailed protocol elsewhere to facilitate the adoption of our method by other investigators. The ability to generate patient-specific A9 DA pacemakers will greatly facilitate research and therapeutic development in Parkinson's disease.

REFERENCES

1. Jimenez-Castellanos J, Graybiel AM. Subdivisions of the dopamine-containing A8-A9-A10 complex identified by their differential mesostriatal innervation of striosomes and extrastriosomal matrix. Neuroscience. 1987;23:223–42.
2. German DC, Manaye KF. Midbrain dopaminergic neurons (nuclei A8, A9, and A10): three-dimensional reconstruction in the rat. J Comp Neurol. 1993;331:297–309.
3. Matsuda W, Furuta T, Nakamura KC, Hioki H, Fujiyama F, Arai R, et al. Single nigrostriatal dopaminergic neurons form widely spread and highly dense axonal arborizations in the neostriatum. J Neurosci. 2009;29:444–53.
4. Damier P, Hirsch EC, Agid Y, Graybiel AM. The substantia nigra of the human brain. II. Patterns of loss of dopamine-containing neurons in Parkinson's disease. Brain. 1999;122:1437–48.
5. Thompson L, Barraud P, Andersson E, Kirik D, Bjorklund A. Identification of dopaminergic neurons of nigral and ventral tegmental area subtypes in grafts of fetal ventral mesencephalon based on cell morphology, protein expression, and efferent projections. J Neurosci. 2005;25:6467–77.
6. McRitchie DA, Hardman CD, Halliday GM. Cytoarchitectural distribution of calcium binding proteins in midbrain dopaminergic regions of rats and humans. J Comp Neurol. 1996;364:121–50.
7. Grealish S, Jonsson ME, Li M, Kirik D, Bjorklund A, Thompson LH. The A9 dopamine neuron component in grafts of ventral mesencephalon is an important determinant for recovery of motor function in a rat model of Parkinson's disease. Brain. 2010;133:482–95.
8. Grace AA, Bunney BS. The control of firing pattern in nigral dopamine neurons: single spike firing. J Neurosci. 1984;4:2866–76.
9. Albin RL, Young AB, Penney JB. The functional anatomy of basal ganglia disorders. Trends Neurosci. 1989;12:366–75.
10. DeLong MR, Benabid AL. Discovery of high-frequency deep brain stimulation for treatment of Parkinson disease: 2014 Lasker Award. JAMA. 2014;312:1093–4.
11. Arenas E, Denham M, Villaescusa JC. How to make a midbrain dopaminergic neuron. Development. 2015;142:1918–36.
12. Chambers SM, Fasano CA, Papapetrou EP, Tomishima M, Sadelain M, Studer L. Highly efficient neural conversion of human ES and iPS cells by dual inhibition of SMAD signaling. Nat Biotechnol. 2009;27:275–80.
13. Bonilla S, Hall AC, Pinto L, Attardo A, Gotz M, Huttner WB, et al. Identification of midbrain floor plate radial glia-like cells as dopaminergic progenitors. Glia. 2008;56:809–20.
14. Ono Y, Nakatani T, Sakamoto Y, Mizuhara E, Minaki Y, Kumai M, et al. Differences in neurogenic potential in floor plate cells along an anteroposterior location: midbrain dopaminergic neurons originate from mesencephalic floor plate cells. Development. 2007;134:3213–25.
15. Ribes V, Briscoe J. Establishing and interpreting graded Sonic Hedgehog signaling during vertebrate neural tube patterning: the role of negative feedback. Cold Spring Harb Perspect Biol. 2009;1:a002014.
16. Bally-Cuif L, Wassef M. Determination events in the nervous system of the vertebrate embryo. Curr Opin Genet Dev. 1995;5:450–8.
17. Fasano CA, Chambers SM, Lee G, Tomishima MJ, Studer L. Efficient derivation of functional floor plate tissue from human embryonic stem cells. Cell Stem Cell. 2010;6:336–47.
18. Kriks S, Shim JW, Piao J, Ganat YM, Wakeman DR, Xie Z, et al. Dopamine neurons derived from human ES cells efficiently engraft in animal models of Parkinson's disease. Nature. 2011.
19. Hobert O. Regulation of terminal differentiation programs in the nervous system. Annu Rev Cell Dev Biol. 2011;27:681–96.
20. Louvi A, Artavanis-Tsakonas S. Notch signalling in vertebrate neural development. Nat Rev Neurosci. 2006;7:93–102.
21. Crawford TQ, Roelink H. The notch response inhibitor DAPT enhances neuronal differentiation in embryonic stem cell-derived embryoid bodies independently of sonic hedgehog signaling. Dev Dyn. 2007;236:886–92.

22. Kirkeby A, Grealish S, Wolf DA, Nelander J, Wood J, Lundblad M, et al. Generation of regionally specified neural progenitors and functional neurons from human embryonic stem cells under defined conditions. Cell Rep. 2012;1:703–14.

23. Qi Y, Zhang XJ, Renier N, Wu Z, Atkin T, Sun Z, et al. Combined small-molecule inhibition accelerates the derivation of functional cortical neurons from human pluripotent stem cells. Nat Biotechnol. 2017;35:154–63.

24. Lepski G, Jannes CE, Nikkhah G, Bischofberger J. cAMP promotes the differentiation of neural progenitor cells in vitro via modulation of voltage-gated calcium channels. Front Cell Neurosci. 2013;7:155.

25. Xi J, Liu Y, Liu H, Chen H, Emborg ME, Zhang SC. Specification of midbrain dopamine neurons from primate pluripotent stem cells. Stem Cells. 2012;30:1655–63.

26. Hu BY, Weick JP, Yu J, Ma LX, Zhang XQ, Thomson JA, et al. Neural differentiation of human induced pluripotent stem cells follows developmental principles but with variable potency. Proc Natl Acad Sci USA. 2010;107:4335–40.

27. Bock C, Kiskinis E, Verstappen G, Gu H, Boulting G, Smith ZD, et al. Reference Maps of human ES and iPS cell variation enable high-throughput characterization of pluripotent cell lines. Cell. 2011;144:439–52.

28. Ohi Y, Qin H, Hong C, Blouin L, Polo JM, Guo T, et al. Incomplete DNA methylation underlies a transcriptional memory of somatic cells in human iPS cells. Nat Cell Biol. 2011;13:541–9.

29. Phanstiel DH, Brumbaugh J, Wenger CD, Tian S, Probasco MD, Bailey DJ, et al. Proteomic and phosphoproteomic comparison of human ES and iPS cells. Nat Methods. 2011;8:821–7.

30. Song B, Cha Y, Ko S, Jeon J, Lee N, Seo H, et al. Human autologous iPSC-derived dopaminergic progenitors restore motor function in Parkinson's disease models. J Clin Invest. 2020;130:904–20.

31. Schweitzer JS, Song B, Herrington TM, Park TY, Lee N, Ko S, et al. Personalized iPSC-derived dopamine progenitor cells for Parkinson's Disease. N. Engl J Med 2020;382:1926–32.

32. Doi D, Samata B, Katsukawa M, Kikuchi T, Morizane A, Ono Y, et al. Isolation of human induced pluripotent stem cell-derived dopaminergic progenitors by cell sorting for successful transplantation. Stem Cell Rep. 2014;2:337–50.

33. Kikuchi T, Morizane A, Doi D, Magotani H, Onoe H, Hayashi T, et al. Human iPS cell-derived dopaminergic neurons function in a primate Parkinson's disease model. Nature. 2017;548:592–6.

34. Kim TW, Piao J, Koo SY, Kriks S, Chung SY, Betel D, et al. Biphasic activation of WNT signaling facilitates the derivation of midbrain dopamine neurons from hESCs for translational use. Cell Stem Cell. 2021;28:343–55.

35. Jovanovic VM, Salti A, Tilleman H, Zega K, Jukic MM, Zou H, et al. BMP/SMAD pathway promotes neurogenesis of midbrain dopaminergic neurons in vivo and in human induced pluripotent and neural stem cells. J Neurosci. 2018;38:1662–76.

36. Jiang H, Ren Y, Yuen EY, Zhong P, Ghaedi M, Hu Z, et al. Parkin controls dopamine utilization in human midbrain dopaminergic neurons derived from induced pluripotent stem cells. Nat Commun. 2012;3:668.

37. Hu Z, Li H, Jiang H, Ren Y, Yu X, Qiu J, et al. Transient inhibition of mTOR in human pluripotent stem cells enables robust formation of mouse-human chimeric embryos. Sci Adv. 2020;6:eaaz0298.

38. Torres EM, Lane EL, Heuer A, Smith GA, Murphy E, Dunnett SB. Increased efficacy of the 6-hydroxydopamine lesion of the median forebrain bundle in small rats, by modification of the stereotaxic coordinates. J Neurosci Methods. 2011;200:29–35.

39. Grealish S, Diguet E, Kirkeby A, Mattsson B, Heuer A, Bramoulle Y, et al. Human ESC-derived dopamine neurons show similar preclinical efficacy and potency to fetal neurons when grafted in a rat model of Parkinson's disease. Cell Stem Cell. 2014;15:653–65.

40. Brown A, Machan JT, Hayes L, Zervas M. Molecular organization and timing of Wnt1 expression define cohorts of midbrain dopamine neuron progenitors in vivo. J Comp Neurol. 2011;519:2978–3000.

41. Sinha S, Chen JK. Purmorphamine activates the Hedgehog pathway by targeting Smoothened. Nat Chem Biol. 2006;2:29–30.

42. Li XJ, Hu BY, Jones SA, Zhang YS, Lavaute T, Du ZW, et al. Directed differentiation of ventral spinal progenitors and motor neurons from human embryonic stem cells by small molecules. Stem Cells. 2008;26:886–93.

43. Jiang H, Xu Z, Zhong P, Ren Y, Liang G, Schilling HA, et al. Cell cycle and p53 gate the direct conversion of human fibroblasts to dopaminergic neurons. Nat Commun. 2015;6:10100.

44. Mercuri NB, Bonci A, Calabresi P, Stratta F, Stefani A, Bernardi G. Effects of dihydropyridine calcium antagonists on rat midbrain dopaminergic neurones. Br J Pharm. 1994;113:831–8.

45. Lacey MG, Mercuri NB, North RA. Two cell types in rat substantia nigra zona compacta distinguished by membrane properties and the actions of dopamine and opioids. J Neurosci. 1989;9:1233–41.

46. Margolis EB, Lock H, Hjelmstad GO, Fields HL. The ventral tegmental area revisited: is there an electrophysiological marker for dopaminergic neurons? J Physiol. 2006;577:907–24.

47. Jones S, Kauer JA. Amphetamine depresses excitatory synaptic transmission via serotonin receptors in the ventral tegmental area. J Neurosci. 1999;19:9780–7.

48. Margolis EB, Lock H, Chefer VI, Shippenberg TS, Hjelmstad GO, Fields HL. Kappa opioids selectively control dopaminergic neurons projecting to the prefrontal cortex. Proc Natl Acad Sci USA. 2006;103:2938–42.

49. Blauwkamp TA, Nigam S, Ardehali R, Weissman IL, Nusse R. Endogenous Wnt signalling in human embryonic stem cells generates an equilibrium of distinct lineage-specified progenitors. Nat Commun. 2012;3:1070.

50. Wakeman DR, Hiller BM, Marmion DJ, McMahon CW, Corbett GT, Mangan KP, et al. Cryopreservation maintains functionality of human iPSC dopamine neurons and rescues Parkinsonian phenotypes in vivo. Stem Cell Rep. 2017;9:149–61.

51. Hartfield EM, Yamasaki-Mann M, Ribeiro Fernandes HJ, Vowles J, James WS, Cowley SA, et al. Physiological characterisation of human iPS-derived dopaminergic neurons. PLoS ONE. 2014;9:e87388.

52. Surmeier DJ, Mercer JN, Chan CS. Autonomous pacemakers in the basal ganglia: who needs excitatory synapses anyway? Curr Opin Neurobiol. 2005;15:312–8.

53. Chan CS, Guzman JN, Ilijic E, Mercer JN, Rick C, Tkatch T, et al. 'Rejuvenation' protects neurons in mouse models of Parkinson's disease. Nature. 2007;447:1081–6.

54. Chan CS, Gertler TS, Surmeier DJ. Calcium homeostasis, selective vulnerability and Parkinson's disease. Trends Neurosci. 2009;32:249–56.

55. Ford CP. The role of D2-autoreceptors in regulating dopamine neuron activity and transmission. Neuroscience. 2014;282:13–22.

56. Giguere N, Delignat-Lavaud B, Herborg F, Voisin A, Li Y, Jacquemet V, et al. Increased vulnerability of nigral dopamine neurons after expansion of their axonal arborization size through D2 dopamine receptor conditional knockout. PLoS Genet. 2019;15:e1008352.

57. Pissadaki EK, Bolam JP. The energy cost of action potential propagation in dopamine neurons: clues to susceptibility in Parkinson's disease. Front Comput Neurosci. 2013;7:13.

58. Piao J, Zabierowski S, Dubose BN, Hill EJ, Navare M, Claros N, et al. Preclinical efficacy and safety of a human embryonic stem cell-derived midbrain dopamine progenitor product, MSK-DA01. Cell Stem Cell. 2021;28:217–29.

59. Parmar M, Grealish S, Henchcliffe C. The future of stem cell therapies for Parkinson disease. Nat Rev Neurosci. 2020;21:103–15.

COMPETING INTERESTS
The authors declare no competing interests.

ADDITIONAL INFORMATION
Supplementary information The online version contains supplementary material available at https://doi.org/10.1038/s41380-022-01628-1.

Correspondence and requests for materials should be addressed to Jian Feng.

Reprints and permission information is available at http://www.nature.com/reprints

Publisher's note Springer Nature remains neutral with regard to jurisdictional claims in published maps and institutional affiliations.